Effect of Al₁₃ Polycation Grafting on Apple Wastes Activated Carbon That Have A Porous Structure

ZOUBIDA MARSA*, CHAFIA BOUCHELTA[1], NASSIMA RAMDANE[1], MED SALAH MEDJRAM[1] and PIERRE MAGRI[2]

[1]Laboratory LGCES, Faculty of Technology, Skikda 20 Août 1955 University, El-Hadaeik Road, P.O. Box 26, 21000, Skikda, Algeria.
[2]Laboratory LCP-A2MC, Lorraine University, 1bd Arago Metz France.
*Corresponding author E-mail address: medjram_ms@yahoo.fr

ABSTRACT

Using physical activation, modified apple wastes with Al₁₃ polycation were utilized such a feedstock's for activated carbon production .thence, The characteristics of synthesized materials were: N_2 adsorption/desorption , Scanning electron microscopy, and Fourier-transform infrared analyses. AS a beginning, one studied the effect of Al₁₃ grafting on textural and chemical surface characteristics of activate,d carbons- Al₁₃ generated . The increasing Al₁₃ content has major inffluences on the porous structure of the prepared activated carbon; it causes more structurale and intensifies the surface zone and the pore volume (484 m^2/g, micropore area of 400 m^2/g and microporous volume of 0.185 cm^3/g is the best surface area).ALSO The methyl orange adsorption performance of the received adsorbent was investigated to identify the role of Al₁₃, especially its particular structure and high positive charge (+7). Adsorption performance of the grafted activated carbon was significantly enhanced. Raising charges at carbons materials surface by Al₁₃ grafting improved the methyl orange adsorption kinetics. The adsorption data was relevant to Langmuir, Freundlich and Temkin models. The results indicated that the adsorption data belonging better to the Langmuir isotherm model. The prepared activated carbon- Al₁₃ founded to be an efficient material for anionic dye removed from wastewater.

Keywords: Apple wastes; modified activated carbon; Al₁₃; Physical activation; Adsorption; Methyl orange.

INTRODUCTION

Activated carbon is regarded as an oldest adsorbent known in air pollution control and wastewater treatment .nevertheless, the use of this adsorbent for depollution processes is considerably restricted because it is very costly . Therefore, researchers are searching the substitution of this expensive adsorbent by a decreased-cost adsorbents prepared from different agricultural,

industrial and local wastes which are abundant and cheap. Many agricultural wastes have been explored as decreased-cost adsorbent. Some of them comprise: cherry stones[1], olive stones[2–5], oil palm stones[6,7], apricot stones[8,9], sugar cane bagasse[10,11], nutshells[12], pecan shells[13–14], date stones[15,16], and peels of many fruits like orange[17], banana[18,19], pomegranate peel[20], yellow passion fruit and mandarin[21], beet pulp[22], grape seed[23], and apple[24]. Apples constitute one of the most plentiful fruits, with a world production of 68.3 million metric tons for 2005. Although, about 12% of the production is destined to the manufacturing of apples juice and cider. In the other hand, the solid residue from pressing apples (apple pulp) represents more than 12 wt% of the fruit. Hence , large quantities of about 0.84 Mt of apple pulp are produced every year all over the world[25]. This by-product has many applications like: antioxidants production[26-28], hydrogen production[29], extraction of lactic acid[30] and pectin[31], animal feed[32], and activated carbons[24].whereas, many studies have been done by Suarez-Garcia et al. for the feasibility of production of activated carbon from apple peel by using the chemical activation with phosphoric acid[24, 33, 34]. Nevertheless, the preparation of activated carbon from apple wastes by physical activation has never been studied previously and especially a preparation of grafted apple wastes activated carbon using Al_{13} polycation in order to improve the surface and structural properties of the original materials. Al_{13} was widely used because of its specific structure, high molecular weight, and high positive charge. The objective of this study is to prepare a modified activated carbon with Al_{13} polycation from apple wastes by using the physical activation process under steam in a fixed-bed reactor. A particular attention has been paid to the effects of grafting Al_{13} on porosity development and on the increase of activated carbon adsorption performance.well, To investigate the effects of Al_{13} on the adsorption performance of the prepared activated carbons, the removal methyl orange (with negative charges) from aqueous solution on the modified decreased-cost adsorbents (with more positive charges after Al_{13} grafting) were learned.in addition the equilibrium of the adsorption was depicted by Temkin,Langmui,Freundlish models.

EXPERIMENTAL

The raw apple wastes(AW)

The wastes of various sorts of Apple were provided from Algerian juice manufactories .for one week ,the primary matter had firstly to be air-dried at room temperature. then dried at 110 °C for about 48 h.Analysis of apple wastes indicated that : pH (4.18), apparent density (0.60 g/cm³), moisture (5.6 %), ash (3.8%) and volatile matter (79%), were implemented.

However inorganic elements was defined by Suarez-Garcia et al. (3.3% in dry weight)[35]. Suarez-Garcia also studied the elemental and the biopolymer
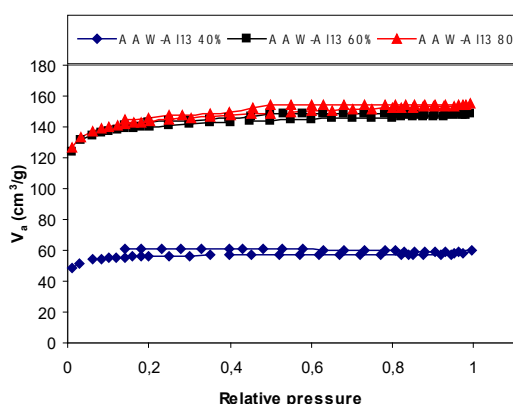
Fig. 1: N$_2$ adsorption-desorption isotherms at -196 °C of apple wastes- Al$_{13}$ activated carbons obtained at different Al$_{13}$ concentrations (40, 60 and 80 wt.%).
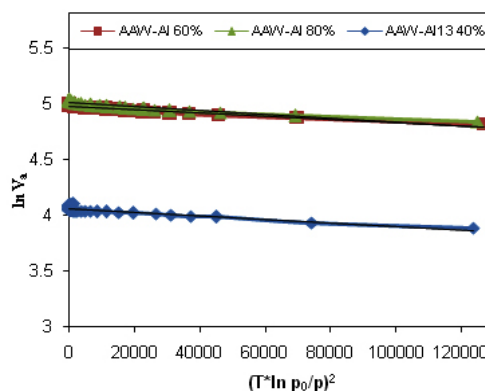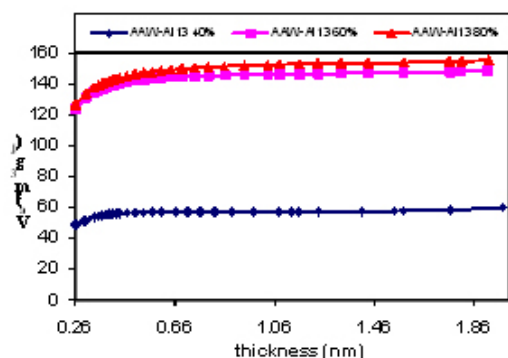

Fig. 2: DR-linear plots for N$_2$ adsorption-desorption isotherms at -196 °C for apple wastes- Al$_{13}$ activated carbons obtained with different Al$_{13}$ concentrations (40, 60 and 80 wt.%).

analysis (wt.%, db.) of apple wastes. The results pointed out that it is formed of 49.56% carbon, 8.43% hydrogen, 38.85% oxygen and 0.97% nitrogen. Respectively The value for hollocellulose and lignin was 44% and 17.3% , 6.7% soluble in organic solvents and 31.3% soluble in water[24, 35]. When we have examined the proximate and chemical analysis of apple wastes, we can deduce that the preparation of activated carbon were promoted by their lignocellulosic composition .

Preparation of Al_{13}

Al_{13} is produced by the hydrolysis of aluminum chloride. This stage is a slow process of hydrolysis with a ranging ratio of OH/Al between 2.2 to 2.8 giving almost a pure solution of the polycation Al_{13}[36-37].

Fig. 3: Curves transformed "t" obtained with Harkins and Jura equation.
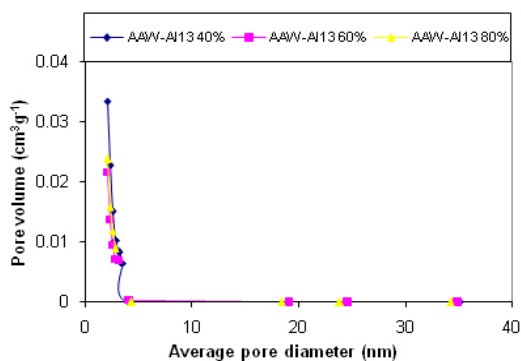
Fig. 4: Pore size distribution for the apple wastes-Al_{13} activated carbons obtained with different Al_{13} concentrations (40, 60 and 80 wt.%).

The solution of Al_{13} was synthesized in laboratory. The experimental procedure was described in our previous works[38-39] by respecting the molar report OH/Al = 2.2. while putting in a beaker in thermostatic bath for 20 minutes at 70 °C, 100 ml of aluminum chloride solution ($AlCl_3 . 6H_2O$) 0.25 M, and by slowly adding of 240 ml of soda solution (NaOH) 0,25 M, with a vigorous agitating and respecting the NaOH flow (2 ml/min), in order to avoid the sursaturation of the hydroxyls ions. Then let cool until 20 °C, with a pH between 5 and 6. Add 280 ml ammonium oxalate 0.1 M, and let precipitate 24 hours. Filter and wash with deionized water. Dry with the free air. Using this standard method, the resulting solution will contain 90-95 % of the polycation Al_{13}. In fact, many studies using the nuclear magnetic resonance spectroscopy (NMR), provided the proof of its existence and allowed the aluminum speciation[40-46].

Preparation of adsorbents

Apple wastes were mixed with Al_{13} polycation solutions prepared at different concentrations (40, 60 and 80 wt.%) in a ratio of 1g of precursor per 4 ml of solution. The impregnated samples were first stirred for 24 h to introduce the polycation in the materials. Then, we used the distilled water to wash the impregnated material several times to dismiss excess electrolytes and dried at 80 °C.

Activated carbons were prepared from modified apple wastes- Al_{13} by pyrolysis under nitrogen flow and activation under water vapour. Pyrolysis of the grafted material was carried out

Table 1: Effect of pyrolysis and activation temperatures on the yield of pyrolysed and activated apple wastes- Al_{13}.

Temperature (°C)		Yield (wt.%)
Pyrolysis	400	39
	500	36
	600	34
	700	33
	800	32
Activation	700	19
	800	15
	900	16

with a horizontal tubular furnace (length of 450 mm and internal diameter of 65 mm). The reactor was a quartz tube (length of 750 mm and internal diameter of 35 mm), which was placed in the furnace. The schematic diagram of the experimental setup was presented in our previous work[47].

Passing to the pyrolysis step, about 10 g of dried apple wastes- Al_{13} (40, 60 and 80 wt. %) were placed in the middle of the reactor .we used different pyrolysis temperatures of 400,500,600, 700 and 800 °C. Nitrogen flow rate was of 100 cm^3 min^{-1} and heating rate was of 10 °C min^{-1} for all the samples. Once the pyrolysis temperature was reached, sample was maintained at this one for 1 h. The resulting works were then physically activated at 800 °C for 4 h under 10 °C $minutes^{-1}$ degree of temperature 100 $cm^3/$ minutes nitrogen circulation degree saturated in steam after passing through the water saturator heated at 80 °C. So, the water partial pressure was of 474 hPa. After activation, the model was cooled to ambient temperature under N_2 flow rate. The received activated carbons are indicated AAW- Al_{13} 40 %, AAW- Al_{13} 60 %, AAW- Al_{13} 80 %.

Characterization

We had examined the raw and activated carbon produced from apple wastes Al_{13} applying nitrogen adsorption-desorption at - 196 °C, Scanning electron microscopy (SEM) and FTIR spectroscopy. The indicators used for determining the maximum activated carbon were the surface area and the porous volume. These values were denoted by adsorption of nitrogen at -196 °C by means of a commercial manometric sorptometer (micrometrics ASAP 2020 Surface Area and Porosity Analyzer). Before the adsorption, the model were out-gassed under vacuum at 200 °C for 3 h. we analyzed adsorption isotherms by using the Brunauer–Emmett–Teller equation (BET) to compute the specific surface area (S_{BET}). The volume of micropore ($V_{DR-\mu}$) was recognized from the Dubinin–Radushkevich equation (DR)[28]. The pore size distribution: BJH adsorption mean pore diameter (Apd_{BJH}), and BJH Adsorption accumulated surface area of pores (S_{BJH-cp}) between 1.7 and 300 nm using the Barrett-Joyner-Halenda (BJH) model we can determine the diameter using the t-method we can calculated the external surface area ($S_t$ext),micropore area (S_{t-u}) and the micropore volume(V_{t-u}) .The cross-sectional area of nitrogen molecule was taken equal to 0.162 nm^2 and the nitrogen adsorbed was regarded as a liquid which has a density of 0.8081 g/cm^3 at -196 °C.

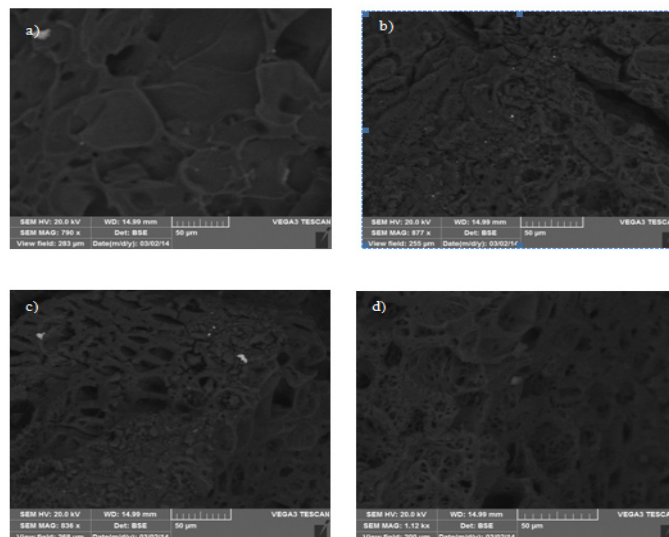The morphology of the materials was examined using scanning electron microscopy (VEGA3 TESCAN).

Fig. 5: Scanning electron micrographs of a) PAW-Al_{13}, b) AAW-Al_{13} 40 %, c) AAW-Al_{13} 60 % and d) AAW-Al_{13} 80 % samples.

Chemical propereties was implemented by FTIR spectroscopy to determine the functional groups at the surface of raw, pyrolysed and activated carbons generated from apple wastes- Al_{13}. Using the KBr wafer technique the infrared transmission spectra were recorded with a Brucker Equinox 55 spectrometer, from 400 to 4000 cm^{-1}. Five hundred scans were taken with a 4 cm^{-1} resolution. Wafers were prepared from the mixture of 0,5 mg of the

Fig. 6: FTIR spectra of natural (AW), pyrolysed apple wastes- Al_{13} (PAW- Al_{13}) and activated apple wastes- Al_{13} with different Al_{13} concentrations (AAW- Al_{13} 60 % and AAW-Al_{13} 80 %).

Fig. 7: Effects of contact time on adsorption of MO dye on AAW-Al_{13} 80 %

sample and 200 mg of KBr. This mixture was condensed in a manual hydraulic press at 59 MPa.

Adsorption studies

Regardless of the Adsorption of methyl orange is considered as the most important important means of assessing removal capacity from the aqueous phase. The efficiency of the dismissal of dye: respectively methyl orange (MO) from aqueous solutions by AAW- Al_{13} 80 % (prepared under the conditions of pyrolysis and activation temperatures of 800 °C during 1 h and 4h for pyrolysis and activation , Nitrogen flow rate of 100 cm^3 min^{-1}, heating rate of 10 °C min^{-1} and 80 wt.% Al_{13} content) was experimentally studied by the way of recording the equilibrium experiments and adsorption isotherms.

Equilibrium studies

In the equilibrium stdy, about 0.1 g of AAW-Al_{13} 80 % activated carbon was directly mixed with 1000 ml of methyl orange (MO) solution and agitated in a mechanical shaker at 200 rpm. In the favour of the determination of equilibrium time, the aqueous samples were taken at reset time intervals, and the concentration C_e (mg/l) of dye leftover in the aqueous phase were measured applying a double beam UV–VIS spectrophotometer (1605 SHIMADZU) at λ_{max} 466 nm.

Adsorption isotherm

Measuredly, Batch adsorption experiments were impemented in 500 ml glass-stoppered flask at a stable temperature (25 °C). About 0.1 g of AAW- Al_{13} 80 % was throughly mixed with 100 ml of methyl orange (MO) solution. The isotherms studies were performed by differing the initial (MO) concentrations from 1.2 to 300 mg/L. The melanges were continuously stirred (200 rpm), for 45 minutes. We have determine previously this equilibrium time from equilibrium experiments.

After such agitation, models of 5 ml were subjected to for analysis using UV-Visible spectrophotometer (1605 SHIMADZU) at λ_{max} 466 nm to determine the residual concentration of dye in the aqueous phase. Using equation (1); the adsorption capacity at time *t*, q_t (mg/g), was calculated .
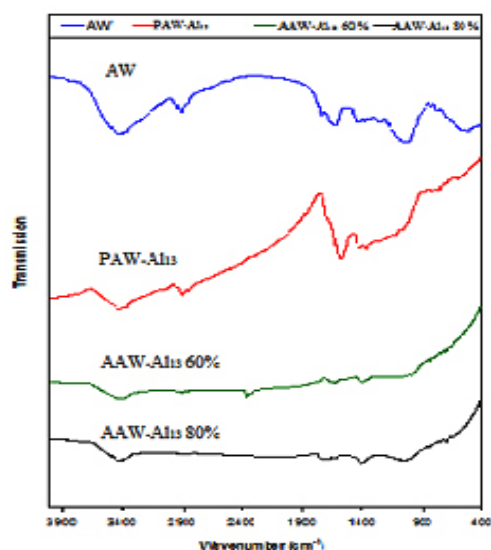
$$q_t = \frac{(C_0 - C_e)V}{m} \qquad ...(1)$$
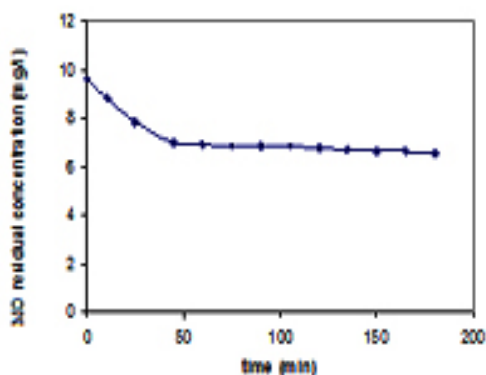
Where C_0 and C_e (mg/L) are the liquid-phase concentrations of dye at initial and any time t, respectively. V is the volume of the solutions (L), and m is the mass of adsorbent used (g).

We have applied three isothermal models to the experimental data[48]. The adsorption isotherm point out how the adsorption molecules distribute between the liquid phase and the solid phase when the adsorption operation reaches an equilibrium state. The analysis of the isotherm data by fitting them to different isotherm models is an important step to find the suitable model that can be used for design objective.

Langmuir sample was applied to the experimental data. The Langmuir isotherm is focus on the estimation that the adsorption process takes place on sites having the same energy and each site can be busied by only one molecule. Besides the interactions between adsorbed ions are neglected. The linear expression for the Langmuir isotherm is:

$$\frac{C_e}{q_e} = \frac{C_e}{q_m} + \frac{1}{K_L q_m} \qquad ...(2)$$

when C_e is the equilibrium concentration of dye (mg/L) and q_e is the quantity of the dye molecules adsorbed (mg/L). q_m and K_L are the maximal adsorption capacity (mg/g) and the Langmuir equilibrium constant (L/g), respectively.

The Freundlich model is an empirical equation estimating that that the adsorption process takes place on a heterogeneous surface through a multilayer adsorption mechanism and adsorption ability is related to the concentration of dyes at equilibrium. The Freundlich model is given by the linear equation:

$$\log q_e = \log K_F + \frac{1}{n} \log C_e \qquad ...(3)$$

When q_e is the amount adsorbed (mg/g), and C_e is the equilibrium concentration of the adsorbate (mg/L). K_F is the Freundlich adsorption constant according to adsorption capacity of the adsorbent (mg/g) and $1/n$ is the adsorption intensity. Values of $n > 1$ represent suitable adsorption condition.

The Temkin model considers the impacts of indirect adsorbate–adsorbente interactions on adsorption, and suggests that the heat of adsorption of all the molecules in the layer would augment linearly with coverage due to these interactions [30]. The linear form of Temkin isotherm is expressed as:

$$qe = B \ln A + B \ln Ce \qquad ...(4)$$

Where B is the Temkin stable is relevant to heat of adsorption. $B = (q_0 RT)/b$, T is the absolute temperature in Kelvin and R is the universal gas constant, 8.314 J. (mol. K)[-1]. The constant b (KJ. mol^{-1}) is related to the heat of adsorption. A is the equilibrium curving constant (L/mg). The constant A and B can be determined by a plot of qe versus ln Ce.

RESULTS and DISCUSSIONS

Determination of the optimal pyrolysis temperature

The product of pyrolysed or/and activated apple wastes- Al_{13} can be determined as the ratio of the mass of pyrolysed or/and activated apple wastes-Al_{13} upon the mass of the raw grafted material.

Pyrolysis experiments at different temperature have been performed in order to determine the temperature at which the yield is the lowest i.e. the failure of mass after pyrolysis is maximal.
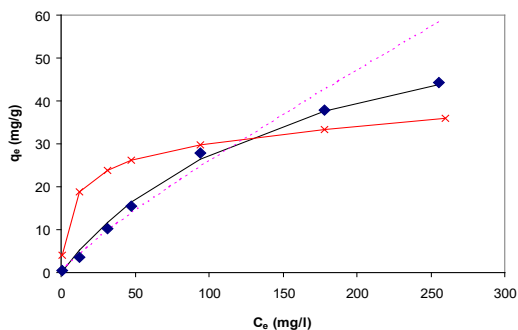
Fig. 8: Modeling of adsorption isotherm of MO on AAW-Al$_{13}$ 80 % [symbols: experiments; solid line: Langmuir model; broken line: Freundlich model; line with symbol: Temkin].

Table 1 indicates that the increase of temperature makes the yield of pyrolysed apple wastes- Al_{13} decreases from 400to 700 °C. This is the result of the partial decomposition of apple wastes. Adapted from a study of Suarez-Garcia et al., four weight loss steps can be identified in the TG/DTG curves of apple pulp[38], the first step happens at 120 °C, and can be attributed to moisture release. A second step occurs at 233 °C, and is attributable to lowering of hemicellulose and organic and/or aqueous extractives. The third step, at 328 °C, would correspond to thermal degradation of cellulose. The last step overlaps with the two last ones and its property temperatures cannot be vary so clearly. This weight loss step, ascribable to lignin degradation, seems with maximal weight loss rate at 406 °C. The lowest yield is obtained between 700 and 800 °C. The optimal pyrolysis temperature is then fixed at 700 °C. All the samples are pyrolysed at this temperature as follows;

Table 1, also informs the results obtained for Al_{13} 80 % grafted samples pyrolysed at 700 °C and activated below steam at various activation temperatures and constant hold time (4 h). Results indicated that the yield minimize after activation, because more volatile maters are released after activation. Indeed, as the activation temperature increases from 700 to 800 °C, the yield of activated carbon reduces. This is attributed to the removal of volatile matters resulting from the decomposition of significant compounds of apple waste i.e. cellulose and hemicellulose. whereas, the decomposition of hemicellulose and cellulose and greafting Al_{13}

polycation improve the pore diffusion and creates porosity in apple wastes that permit a better diffusion of oxygen into the particles. Thus, lignin, the third component of apple wastes, which the decomposition is more difficult, can better react with the oxidizing agent. At 900 °C, the yield increase slightly. Activation of apple wastes at increasing heat does not lead to a decreased yield.

N$_2$ adsorption-desorption isotherms

Figures 1-4 disclose the form and behavior of the N$_2$ adsorption-desorption isotherms, of the t- and DR-plots, and the micropore size distribution from BJH sample, for the series of apple wastes- Al_{13} activated carbons (40, 60 and 80 % Al_{13} content). Table 2 resumes the values of the structural parameters which characterize the porous structure of the samples, derived from the N$_2$ adsorption-desorption isotherms at -196 °C.

Figure 1 pointed out the N$_2$ adsorption-desorption isotherms at -196 °C, on apple wastes- Al_{13} activated carbons obtained with different Al_{13} concentrations (40, 60 and 80 wt.%). All the adsorption isotherms have the type I shape typical for materials with a well-developed microporosity. whereas, a small upward curving at high relative pressure denote that some meso- and/or macropores are evolved inside activated carbon obtained at 60 and 80 % Al_{13} content.

However, the DR-plots (Figure 2) implys a type C behavior, with a small upward bending at high pressures, corresponding to low values of $(T*\ln p_0/p)^2$ which results from adsorption in meso and/or macropores.

The t-plots (Figure 3) indicates that from a thickness (computed by Harkins and Jura equation), we can deduce the particular external area (S_{t-ext}) responsible of multilayer adsorption, which characterised type II isotherm besides to type I isotherm. The values of the external area (S_{t-ext}) increase gradually with the increase of Al_{13} content from 40 to 80 % because the polycation is fixed at the surface and introduced in the porous structure after pyrolysis and activation, so, more specific surface is developed in the materials.

Table 2. Textural parameters deduced from N$_2$ adsorption at -196 °C on apple wastes- Al_{13} activated carbons prepared with different Al_{13} concentrations (40, 60 and 80 wt.%).

Samples	AAW-Al_{13} 40 %	AAW-Al_{13} 60 %	AAW-Al_{13} 80 %
S_{BET} (m^2 g^{-1})	189	471	484
$V_{DR-\mu}$ (cm^3 g^{-1})	0.047	0.167	0.169
S_{t-ext} (m^2 g^{-1})	27	73	84
$S_{t-\mu}$ (m^2 g^{-1})	162	398	400
$V_{t-\mu}$ (cm^3 g^{-1})	0.075	0.184	0.186
S_{BJH-cp} (m^2 g^{-1})	10.55	38.65	47.92
Apd_{BJH} (nm)	1.96	1.95	1.98

The distribution of Pore extent is regarded to be a good indicator of the uniformity of porous materials. Figure 4 show the pore extent distributions of activated carbons from apple wastes- Al_{13} obtained at different Al_{13} concentrations (40, 60 and 80 wt.%). The great augmentation of all pore extent distribution bending for pore diameters of about 2 (nm) indicated the formation of relatively uniform micropores in majority of the structure of the activated materials as stated by the classification adopted by the International Union of Pure and Applied Chemistry (IUPAC). This augmentation came to be significant in the grafted activated carbons prepared with 60 and 80 % of Al_{13}. In fact, the values of ($V_{DR-\mu}$), ($V_{t-\mu}$) and ($S_{t-\mu}$) and (S_{BET}) presented in Table 2 are higher for AAW- Al_{13} 60 % and AAW- Al_{13} 80 %. Nevertheless, only a tiny increase is observed in the values of these parameters at 80 wt.% of Al_{13}. For all the samples, the BJH average pore diameters (Apd_{BJH}) are closer to 2 nm.

From the derived textural data (see Table 2) it copmlys that the increase in Al_{13} content from 40 to 60 % causes an important development in the surface area and porosity of the prepared samples. Hence; This phenomenon signes that the Al_{13} species essentially contributed to the remarkable improvement of the surface areas of the modified apple wastes activated carbons. When the Al_{13} species were introduced into the apple wastes under high activation temperature, the compounds of apple wastes hemicellulose, cellulose and lignin are decomposed under the activating action of $H_2O + N_2$, so the native cations were replaced by polyaluminum. Higher Al_{13} content favor the occupation of more sites and consequently increased the surface area.

Conserning the three prepared activated carbons, we noticed ordinarily that the values of the micropore area ($S_{t-\mu}$) are greater than the values of the external area (S_{t-ext}) because these activated

Table 3: Assignments of IR absorption bands for AW, PAW- Al_{13}, AAW- Al_{13} 60 % and AAW- Al_{13} 80 %.

σ (cm⁻¹)	Assignment	Comment
3400	ν (O-H)	Stretching in hydroxyl groups
2910	ν_{as} (C–H)	Stretching in alkyl groups
2840	ν_s (C–H)	Stretching in alkyl groups
1740	ν (C=O)	Stretching in esters[38-39]
1640	ν (C=C)	Aromatic skeletal stretching bands
1580	ν (C=C)	Assigned to skeletal stretch in condensed aromatic system
1430	δ (CH₂)	Stretching in ester[39]
1375	δ (C-H)	C-H Asymetric and symetric bending
1336	δ (C-H)	C-H Asymetric bending[39]
1240	ν_{as} (C-O)	Stretching of aromatic ethers, ester and phenols
1150	ν (C-O-C), ν (C=C), methoxyl–O–CH₃	Stretching vibration in pyranose ring skeletal or stretching in aromatic ring
1060	ν (C-O), ν (C-C), δ (OCH)	C-O, C-C and OCH stretching
1035	ν (C-O)	Stretching in alcohol
826-743-690	δ (C-H)	Aromatic C–H out-of-plane bending vibrations Al-OH-Al stretching
984		Al-OOH
807		Al-OH
715		Stretching in C–C
400-600	ν (C-C)	

σ is the wave number.

carbons exhibited type I adsorption isotherms typical of predominant microporous structure.*3.3. Scanning electron microscopy*

Figure 5 pointed out that:the Scanning electron micrographs accomplished on pyrolysed apple wastes-Al_{13} (PAW-Al_{13}) and activated apple wastes- Al_{13} with different Al_{13} concentrations (40, 60 and 80 wt.%). (AAW-Al_{13} 40 %, AAW-Al_{13} 60 % and AAW-Al_{13} 80 %) . The study of the pyrolysed apple wastes-Al_{13} structure (Figure 5.a) points out the presence of a few macropores of various size and geometry. Whereas, the augmentation of Al_{13} concentrations (Figure 5.b, 5.c, 5.d) create gradual and more regular macroporosity in the materials structures.

Figure 6 pointed out that: The FTIR spectra of natural, pyrolysed and activated apple wastes grafted with Al_{13} and the assignments of IR absorption bands are gathered in Table 3.Also The IR spectrum of natural apple wastes agrees with the results of Suarez-Garcia et al.[49]. This later used infrared spectroscopy in order to compare the behaviour of apple pulp, alone and impregnated with 60 wt.% H_3PO_4. The assignment of absorption bands indicates that the functional groups carboxyl, ester, aromatic, alcohol, alkene, hydroxyl, ether and carboxyl are ubiquitous in the raw material. That is

Table 4: Langmuir, Freundlich and Temkin parameters for the adsorption of MO on AAW-Al_{13} 80 %.

Models Parameters	*MO*
Langmuir	
q_m (mg/g)	71
K_L (L/mg)	0.062
R^2	0.98
Freundlich	
K_F (mg/g)	0.55
n	1.22
R^2	0.95
Temkin	
A (L/mg)	1.48
B	6.43
b ($KJ.mol^{-1}$)	32
R^2	0.85

in conformity with the composition of apple wastes, which are essentially comprised of : hemicelluloses, lignin and, cellulose,.

IR Spectra obtained for pyrolysed apple wastes-Al_{13} pointed out that after carbonisation under nitrogen flow, the bands at 3400, 2910, 2840, 1740 and 1035 cm^{-1} initially present in the raw material disappear. This indicates a decrease of water and aliphatic compound contents. New band appears at 1580 cm^{-1}. This band is assigned to C=C skeletal stretch in condensed aromatic system[49]. This indicates an increase of aromaticity during pyrolysis, which is probably due to the decomposition or cocking of several unsaturated chemical structures.

After activation, the IR absorption bands exhibit a lower intensity than after pyrolysis. This change in intensity is the result of (i) the activating action of $H_2O + N_2$ at high temperature, oxygen and hydrogen groups are decomposed and extracted from the surface and (ii) to the introduction of Al_{13} species in the activated apple wastes surface.

Capacity of Adsorption of methyl orange studies of equilibrium

Figure 7pointed out that: the impact of contact time on batch adsorption of MO on AAW-Al_{13} 80 %. Adsorption of the studied dye can be dpicted by a two stage kinetic behaviour, the first with a rapid initial dye adsorption between 1 and 45 minutes followed later on by a much slower rate. The second augments in contact time has a negligible effect on the quantities of adsorption. This phenomenon can be explained as follow: during adsorption of dyes, principally the dye molecules arrived to the boundary layer, afterward they had to disperse into the adsorbent surface, and finally, they had to disperse into the porous structure of adsorbent. Therefore, this phenomenon will take a relatively longer contact time. According to these results, the contact time was fixed at 45 minutes.

Adsorption isotherms

The Adsorption isotherm of MO on AAW-Al_{13} 80 % is indicated in Figure 8. The obtained isotherm was part of type I, that is given by microporous adsorbents with a relatively tiny external surface. Maximal dye adsorption ability determined

at the plateau of the isotherm is 71 mg/g. The highly improved capacity of AAW-Al$_{13}$ 80 % may be attributed to its large BET surface area, micropore surface area, the high positive charge and micropore volume of Al$_{13}$ species that induce certainly higher electrostatic attractions for MO negative charges.

Using Freundlish, and Temkin models) figure 8) The equilibrium adsorption data were interpreted). Values of Langmuir, Freundlich and Temkin parameters are mentioned in Table 4.

Figure 8 indicated that there is an acceptable adaptation between experiments and Langmuir model . The comparison of correlation coefficients (R^2) of the linearized form of both equations mentions that the Langmuir model yield a better fit for the experimental equilibrium adsorption data than the Freundlich and Temkin models. This proposes the monolayer coverage of the surface of the studied activated carbons. The *n* value in Freundlich model were superior to 1 (*n* > 1), indicating a good adsorption of MO on the prepared activated carbon.

Conclusion

This work shows that modified apple wastes with Al$_{13}$ polycation can be used as precursor to produce activated carbon with a rather well-developed porosity by pyrolysis and physical activation using water vapour. The conditions of 80 % Al$_{13}$ concentration, 700 °C pyrolysis temperature for 1 h hold time with a 10 °C min^{-1} heating rate below   100 cm^3 min^{-1} nitrogen flowing rate, and 800 °C activation temperature for 4 h hold time are sufficient to produce an adsorbent with BET surface area of 484 m^2/g and micropore volume of 0.17 cm^3 g^{-1}.   The yield of activated carbon is conversely related to pyrolysis and activation temperatures. SEM examination of pyrolysed and activated apple wastes-Al$_{13}$ shows that the porosity became more uniform and increases gradually with increasing in Al$_{13}$ content. Nitrogen adsorption indicated that the activated carbons received are initially microporous. Thence, FTIR spectroscopy pointed out that many oxygen-containing functional groups are existed in the raw material while aromatic structures are enhanced after pyrolysis and activation. Activated carbon prepared from apple wastes- Al$_{13}$ 80 % was utilized as an adsorbent for dismissing methyl orange from aqueous solution. The maximum adsorption capacity for MO dye on the prepared activated carbon was arrived after 45 min and was 71 mg/g. Hence ,the positive charge of the grafted polycation promotes the elimination of the anionic dye from water. The equilibrium data fitted well in the Langmuir model of adsorption, implying homogeneous and monolayer adsorption.

REFERENCES

1.   Duran-Valle, J.C.; Gomez-Corzo, M.; Pastor-Villegas, J.; Gomez-Serrano, V.; *Study of cherry stones as row material in preparation of carbonaceous adsorbents, J. Anal. Appl. Pyrolysis* **2005**, *73,* 59–67.

2.   Martinez, M.L.; Torres, M.M.; Guzman, C.A.; Maestri, D.M.; *Preparation and charachteristics of activated carbon from olive stones and walnut shells, Ind. Crops Prod.* **2006**, *23,* 23–28.

3.   Rios, R.V.R.A.; Martinez-Escandell, M.; Molina-Sabio, M.; Rodriguez- Reinoso, F.; *Carbon foam prepared by pyrolysis of olive stones under steam, Carbon* **2006**, *44,* 1448–1454.

4.   El-Sheikh, A.H.; Newman, A.P.; Al-Daffaee, H.K.; Phull, S.; Cresswell, N.; *Characterization of activated carbon prepared from a single cultivar of Jordanian Olive stones by chemical and physicochemical techniques, J. Anal. Appl. Pyrolysis* **2004**, *71,* 151–164.

5.   Gonzalez, M.T.; Rodrgljez-Reinoso, F.; Garcia, A.N.; Marcilla, A.; *CO$_2$ activation of olive stones carbonized under different experimental conditions, Carbon* **1997**, *35 (1)* 159–165.

6.   Guo, J.; Lua, A.C.; *Activated carbon prepared from oil palm stone by one-step CO$_2$ activation for gaseous pollutant removal, Carbon* **2000**, *38,* 1985–1993.

7.   Guo, J.; Lua, A.C.; *Textural and chemical characterisations of activated carbon prepared from oil-palm stone with H$_2$SO$_4$ and KOH impregnation, Microporous Mesoporous*

Mater. **1999**, *32,* 111–117.

8. Sentorun-Shalaby, C.; Ucak-Astarlýoglu, M.G.; Artok, L.; Sarici, C.; *Preparation and characterisation of activated carbons by one-step steam pyrolysis/activation from abricot sotones, Microporous Mesoporous Mater.* **2006,** *88,* 126–134.

9. Gergova, K.; Eser, S.; *Effects of activation method on the pore structure of activated carbons from apricot stones, Carbon* 1996, *34 (7),* 879–888.

10. Ahmedna, M.; Marshall, W. E.; Rao, R. M.; *Surface properties of granular activated carbons from agricultural by-products and their effects on raw sugar decolorization, Bioresour. Technol.* **2000**, *71,* 103-112.

11. Tsai, W. T.; Lee, M. K.; Chang, Y. M.; *Fast pyrolysis of rice straw, sugarcane bagasse and coconut shell in an induction-heating reactor, J. Anal. Appl. Pyrolysis* **2006**, *76,* 230–237.

12. Dawson, E.A.; Parkes, G.M.B.; Barnes, P.A.; Chinn, M.J.; *An investigation of the porosity of carbons prepared by constant rate activation in air, Carbon* **2003,** *41,* 571–578.

13. Guo, Y.; Rockstraw, D.A.; *Physicochemical properties of carbons prepared from pecan shell by phosphoric acid activation, Bioresour. Technol.* **2007**, *98,* 1513–1521.

14. Ng, C.; Marshall, W.E.; Rao, R.M.; Bansode, R.R.; Losso, J.N.; *Activated carbon from pecan shell: process description and economic analysis, Ind. Crops Prod.* **2003**, *17,* 209-217.

15. Haimour, N.M.; Emeish, S.; *Utilisation of date stones for production of activated carbon using phosphorique acid, Waste Manage.* **2006**, *26 ,* 651–660.

16. Girgis, B.S.; El-Hendawy, A.; *Porosity development in activated carbons obtained from date pits under chemical activation with phosphoric acid, Microporous Mesoporous Mater.* **2002,** *52 ,* 105–117.

17. Rosas, J.M.; Bedia, J.; Rodriguez-Mirasol, J.; Cordero, T.; *On the preparation and characterisation of chars and activated carbons from orange skin, Fuel Process. Technol* **2010**, *91,* 1345-1354.

18. Achak, M.; Hafidi, A.; Ouazzani, N.; Sayadi, S., Mandi, L.; *Low cost biosorbent "banana peel" for the removal of phenolic compounds from olive mill wastewater: Kinetic and equilibrium studies, J. Hazard. Mater***2009**, *166,* 117–125.

19. Kadirvelu, K.; Kavipriya, M.; Karthika, C.; Radhika, M.; Vennilamani, N.; Pattabhi, S.; *Utilization of various agricultural wastes for activated carbon preparation and application for the removal of dyes and metal ions from aqueous solutions, Bioresour. Technol.* **2003**, *87,* 129–132.

20. Kamal Amin, N.; *Removal of direct blue-106 dye from aqueous solution using new activated carbons developed from pomegranate peel: Adsorption equilibrium and kinetics, J. Hazard. Mater.* **2009**, *165,* 52–62.

21. Pavan, F. A.; Gushikem, Y.;. Mazzocato, A. C.; Dias, S. L.P.; Lima, E. C.; *Statistical design of experiments as a tool for optimizing the batch conditions to methylene blue biosorption on yellow passion fruit and mandarin peels, Dyes Pigments* **2007**, *72,* 256-266.

22. Mudoga, H. L.; Yucel, H.; Kincal, N.S.; *Decolorization of sugar syrups using commercial and sugar beet pulp based activated carbons, Bioresour. Technol.* **2008**, *99* 3528–3533.

23. Ozçimen, D.; Ersoy-Meriçboyu, A.; *Removal of copper from aqueous solutions by adsorption onto chestnut shell and grapeseed activated carbons, J. Hazard. Mater.* **2009**, *168,* 1118–1125.

24. Suarez-Garcia, F.; Martinez-Alonso, A.; Tascon, J.M.D.; *Pyrolysis of apple pulp: effect of operation conditions and chemical additives, J. Anal. Appl. Pyrolysis* **2002,** *62,* 93–109.

25. Bhatnagar, A.; Sillanpaa, M., *Utilization of agro-industrial and municipal waste materials as potential adsorbents for water treatment-A review, Chem. Eng. J.* **2010**, *157* 277–296.

26. Virot, M.; Tomao, V.; Le Bourvellec, C.; Renard, C.M.C.G.; Chemat, F.; *Towards the industrial production of antioxidants from food processing by-products with ultrasound-assisted extraction, Ultrasonics Sonochem.* **2010,** *17,* 1066–1074.

27. Wijngaard, H. H., Brunton, N.; *The optimisation of solid–liquid extraction of antioxidants*

from apple pomace by response surface
methodology, *J. Food Eng.* **2010**, *96,* 134–
140.

28.   Suarez, B.; Alvarez, A.L.; Garcia, Y.D.;
del Barrio, G.; Picinelli Lobo, A.; Parra, F.;
*Phenolic profiles, antioxidant activity and in
vitro antiviral properties of apple pomace,
Food Chem.* **2010**, *120,* 339–342.

29.   Doi, T.; Matsumoto, H.; Abe, J.; Morita, S.;
*Application of rice rhizosphere microflora for
hydrogen production from apple pomace,
International journal of hydrogen energy*
2010, *35,* 7369-7376.

30.   Gullon, B.; Yanez, R.; Alonso, J.L.; Parajo, J.C.;
*Lactic acid production from apple pomace
by sequential hydrolysis and fermentation,
Bioressource technology* **2008**, *99,* 308-
319.

31.   Kumar, A.; Chauhan, G.S.; *Extraction and
characterization of pectin from apple pomace
and its evaluation as lipase (steapsin) inhibitor,
Carbohydrate Polymers* **2010**, *82,* 454–459.

32.   Joshi, V.K.; Sandhu, D.K.; *Preparation and
evaluation of an animal feed by-product
produced by solid-state fermentation of apple
pomace, Bioresour. Technol.* **1996**, *56,* 251-
255.

33.   Suarez-Garcia, F.; Martinez-Alonso, A.;
Tascon, J.M.D.;   *Pyrolysis of apple pulp:
chemical activation with phosphoric acid, J.
Anal. Appl. Pyrolysis* **2002**, *63,* 283–301.

34.   Suarez-Garcia, F.; Martinez-Alonso, A.;.
Tascon, J.M.D.; *Porous texture of activated
carbons prepared by phosphoric acid
activation of apple pulp, Letters to the editor
/ Carbon* **2001,** *39 ,*1103 –1116.

35.   Suarez-Garcia, F.; Martinez-Alonso, A.;
Fernandez Ilorent, M.; Tascon, J.M.D.;
*Inorganic matter characterization in vegetable
biomass feedstocks, Fuel* **2002**, *81,* 1161-
1169.

36.   Ohtsuka, Kunio.; *Preparation and Properties
of Two-Dimensional Microporous Pillared
Interlayered Solids / Chem. Mater.* **2001**, *13*,
704-710.

37.   Liang-guo Yan, Xiao-quan Shan, *Adsorption
of cadmium onto Al13-pillared acid-activated
montmorillonite / Journal of Hazardous
Materials* **2008**, *156,* 499–508.

38.   Marsa, Z.; Ramdane, N.; Maghzili, B.; Rogalski,

M.; Bouchelta, C.; Medjram, M.S.; Soltane,
M.; *Comparative study of the adsorption
of phenol on Al13 and the bentonite from
Mostagh-Algeria, Phys. Chem. News* **2012**,
64, 69-75.

39.   Marsa, Z. ; Ramdane, N. ; Medjram, M.S. ;
Maghzili, B. ; Rogalski. M. ; Bouchelta, C.;
Soltane. M.; *Study of the adsorption of phenol
on polycation Al13, Scientical environnement
et santé* **2014,** *1 1281,* 1-5.

40.   Ohtsuka, Kunio.; and Hayashi, Yoshimasa.;
*Incorporation of Low-dimensional Materials
into the Two-dimensional Interlamellar
Nanospace of a Pillared Interlayered Solid /
Chem. Mater.* **2001**, *13*, 704-710

41.   Furrer, Gerhard.; Gfeller, Michael.; and Wehrli,
Bernhard.; *On the chemistry of the Keggin
Al13 polymer: Kinetics of proton-promoted
decomposition / Geochimica et Cosmochimica
Acta,* **1999,** *63, 19/20 ,* 3069–3076.

42.   Wang, Shan Li.; Wang, Ming, K.; Yu Min,
Tzou.; *Effect of temperatures on formation
and transformation of hydrolytic aluminum
in aqueous solutions / Colloids and Surfaces
A: Physicochem. Eng. Aspects* **2003**, *231,*
143–157.

43.   Zhaoyang, Chen.; Zhaokun, Luan.; Zhiping,
Jia,; Xiaosen, Li.; *Study on the hydrolysis/
precipitation behavior of Keggin Al$_{13}$ and Al$_{30}$
polymers in polyaluminum solutions / Journal
of Environmental Management* **2009**, *90,*
2831–2840.

44.   Kazparda, V.; Lartigesa, B.S.; Frochotb, C.;
d'Espinose de la Cailleriec, J.B.; Viriotb, M.L.;
Portald, J.M.; Gornera, T.; Bersillona, J.L.;
*Fate of coagulant species and conformational
effects during the aggregation of a model of
a humic substance with Al13
polycations / Water Research* **2006**, *40,* 1965
– 1974.

45.   Molis, E.; Thomas, F.; Bottero, J. Y.; Barres,
O.; Masion, A.; *Chemical and Structural
Transformation of Aggregated Al$_{13}$ Polycations,
Promoted by Salicylate Ligand Langmuir*
1996, *12*, 3195-3200.

46.   Shou, Zhao.; Chenghong, Feng.; Xiangning,
Huang.; Baohua, Li.; Junfeng, Niu.; Zhenyao,
Shen.; *Role of uniform pore structure and high
positive charges in the arsenate adsorption
performance of Al13-modified montmorillonite,*

Journal of Hazardous Materials **2012**, *203–204*, 317– 325.

47.   Bouchelta,C.; Medjram, M.S.; Bertrand, O.; Bellat, J.P.; *Preparation and characterization of activated carbon from date stones by physical activation with steam, J. Anal. Appl. Pyrolysis* **2008**, *82,* 70–77.   [48. D o , D. D.; *Adsorption Analysis : Equilibria and Kinetics. Imperial College Press, London,* **1998.**

49.   Suarez-Garcia, F.; Martinez-Alonso, A.;

Tascon, J.M.D.; *A comparative study of the thermal decomposition of apple pulp in the absence and presence of phosphoric acid, Polymer Degradation and Stability* **2002**, *75,* 375–383.

50.   Wilson, H.R.; Smith, C.A.; Kacurakova, M.; Saunders, K.P.; Wellnet, N.; *The mechanical properties and molecular dynamics of plant cell wall polysaccharid studied by Fourier-Transform Infrared Spectroscopy, Plant Physiol.* **2000**, *124 (1),* 397–406.